High power red-light GaInP/AlGaInP laser diodes with nonabsorbing windows based on Zn diffusion-induced quantum well intermixing

Kai Zheng (郑 凯), Tao Lin (林 涛), Li Jiang (江 李), Jun Wang (王 俊), Suping Liu (刘素平), Xin Wei (韦 欣), Guangze Zhang (张广泽), and Xiaoyu Ma (马骁宇)

National Engineering Research Center for Opto-Electronic Device, Institute of Semiconductors, Chinese Academy of Sciences, Beijing 100083

Received August 10, 2005

The layer structure of GaInP/AlGaInP quantum well laser diodes (LDs) was grown on GaAs substrate using low-pressure metalorganic chemical vapor deposition (LP-MOCVD) technique. In order to improve the catastrophic optical damage (COD) level of devices, a nonabsorbing window (NAW), which was based on Zn diffusion-induced quantum well intermixing, was fabricated near the both ends of the cavities. Zn diffusions were respectively carried out at 480, 500, 520, 540, and 580 °C for 20 minutes. The largest energy blue shift of 189.1 meV was observed in the window regions at 580 °C. When the blue shift was 24.7 meV at 480 °C, the COD power for the window LD was 86.7% higher than the conventional LD.

OCIS codes: 140.5960, 140.2020, 140.7300.

High power AlGaInP visible-light laser diodes (LDs) have been promising light sources for high density optical memory systems, high speed laser beam printers, and pumped light source for solid-state lasers and erbium-doped fiber amplifiers. Moreover, a large market potential is medical applications for dermatology, ophthalmology, and photodynamic therapy[1,2]. For high power laser, catastrophic optical damage (COD) is a major factor limiting the maximum output power. COD effect is due to a positive-feedback loop between light absorption and band-gap reduction near the facets, where the process of the absorbed energy accumulating leads to thermal damage of the facet. In order to improve COD level, two methods have been used. One is to reduce the power density at the facets, which can be solved through optimizing active region materials and waveguide structures, for example, exponential shaped flared stripes[3], bent waveguide[4], and large optical cavity[1]. The other is to reduce the light absorption and the defects near the facets. Several approaches have been pursued to reduce the light absorption and the defects near the facets, such as facets coating, non-injection windows[5,6], sulfur passivation of facets[7], and nonabsorbing windows (NAWs). NAW is an effective method to reduce the light absorption near facets by increasing the effective bandgap near facets, and the windows can be realized through etching and regrowth[8,9], Zn or Si impurities diffusion-induced disordering of active region[10−12], and melt back process in liquid phase epitaxial (LPE) growth[13]. In this letter, we demonstrate improved performance of the GaInP/AlGaInP LD with NAW based on Zn diffusion-induced quantum well intermixing (QWI). For comparison, the performance of the LD without NAW will be shown. In addition, the diffused epitaxial wafers under various diffusion temperatures were subjected to room-temperature (297 K) photoluminescence (PL) measurements.

Epitaxial growth was carried out in an AIX-200 R&D system with a horizontal reactor. The growth temperature was 705—725 °C, and reactor pressure was 100 mbar. The source materials were trimethylgallium (TMGa), trimethylindium (TMIn), trimethyaluminum (TMAl), arsine (AsH_3), and phosphine (PH_3). The p-type dopant was Diethylzinc (DEZn), and the n-type dopant was silane (SiH_4). The carrier gas was palladium-diffused hydrogen. The epitaxial layers were grown on a n-doped (100) GaAs substrate with a misorietation of 6° towards (111)A to suppress spontaneous ordering of AlGaInP epitaxial layer[1,14]. All layers include the following sequence from the substrates: a Si-doped 76-nm-thick n-GaInP buffer layer, a Si-doped 1100-nm-thick n-$Al_{0.5}In_{0.5}P$ cladding layer (dopant concentration $n = 5 - 8 \times 10^{17}$ cm^{-3}), a compressively strained single-quantum-well (SQW) structure [barrier: AlGaInP = 16 nm, well: GaInP = 13.8 nm ($\Delta a/a = +1\%$)] between two 104-nm-thick $(Al_{0.55}Ga_{0.45})_{0.5}In_{0.5}P$ waveguide layers, a Zn-doped 1100-nm-thick $Al_{0.5}In_{0.5}P$ cladding layer (dopant concentration $p = 1 - 2 \times 10^{18}$ cm^{-3}), and a higher p-doped contact layers (dopant concentration $p = 1 - 2 \times 10^{20}$ cm^{-3}) including a 100-nm-thick $Ga_{0.5}In_{0.5}P$ layer and a 260-nm-thick GaAs layer.

Samples (a), (b), (c), (d), and (e) were selected from the same epitaxial wafer. Non-diffused regions of all the samples were covered with a 200-nm-thick SiO_2 film so that Zn can only diffuse into the window regions. All the samples were put into sealed quartz ampoules, and 18-mg solid Zn_3As_2 alloy was used as diffusion resources. Diffusion procedures were finished in a box-type furnace and the temperature was detected by a platinum rhodium thermocouple. Samples (a), (b), (c), (d), and (e) were diffused at 580, 540, 520, 500, 480 °C, respectively, for the same diffusion time of 20 minutes. In order to measure PL spectra of the GaInP/AlGaInP active layer, the SiO_2 layers and top layers of all samples were removed. Figure 1 shows the PL energy shifts

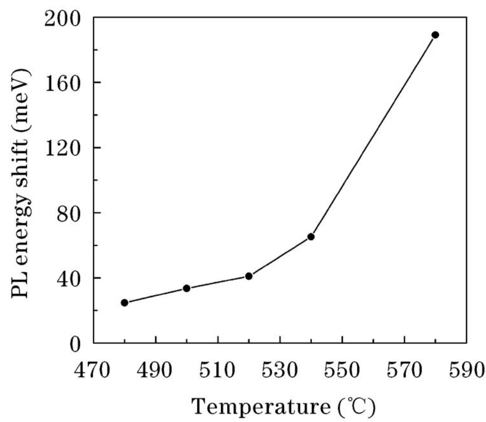

Fig. 1. PL energy shift obtained for the InGaP/AlGaInP quantum well in the Zn-diffused regions as a function of the Zn diffusion temperature. Diffusion time is 20 minutes.

obtained for the GaInP/AlGaInP quantum well in the Zn-diffused regions as a function of the Zn diffusion temperature. And the band gap shifts rapidly increase with increasing Zn diffusion temperature. The maximum PL energy shift of 189.1 meV caused by Zn diffusion was obtained at 580 °C. As the diffusion temperature decreased to 480 °C the energy blue shift reduced to 24.7 meV. When Zn impurities were introduced into the active region in the diffusion process, they were able to enhance the Al-Ga interdiffusion in the heterointerfaces, which induced the composition change of the group-III species in quantum wells and barrier layers near facets[15].

Figure 2 shows the PL peak intensities and the full-width at half-maximum wave (FWHM) of the PL spectra in the diffused regions as a function of the Zn diffusion temperature. It can been seen that although the PL energy shift obtained for the diffused regions gets to the maximum at 580 °C, the PL spectrum gets the least peak intensity and the widest FWHM. It was due to the deterioration of the crystal quality near the window regions. When more Zn atoms diffused into the active layer, more impurities and defects were introduced in the window region, and these impurities and defects would act as non-radiation recombination centers when current was injected. As the diffusion temperature decreased, the amount of the PL energy shift reduced with

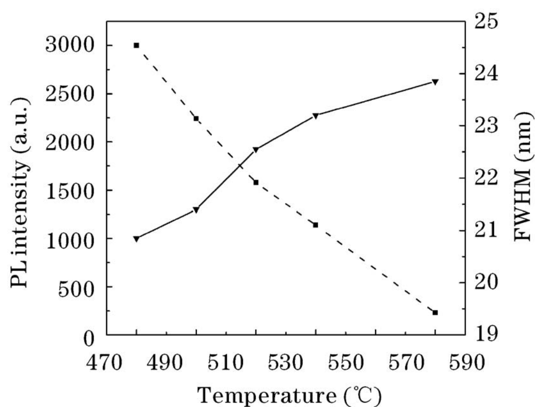

Fig. 2. PL peak intensity (dashed line) and the FWHM (solid line) of the PL spectrum in the diffused regions as a function of the Zn diffusion temperature.

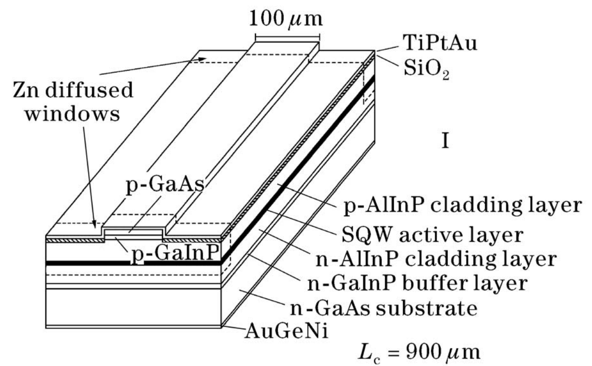

Fig. 3. Schematic diagram of the GaInP/AlGaInP LDs with NAW.

increasing the PL peak intensity and the narrowing of the PL FWHM. Although the PL energy shifts of the diffused regions were less than 44.0 meV at 520 and 500 °C, the low PL peak intensities and the wide PL FWHMs were not suitable for processing into devices. However, the PL energy shift obtained for the sample diffused at 480 °C was 24.7 meV, and the PL spectrum was clear and sharp, indicating high structural and optical quality. This wafer was used to fabricate devices, and the characteristics of the laser diodes would be discussed below.

Figure 3 shows the schematic diagram of the GaInP/AlGaInP LDs with NAW, which has an oxide stripe broad area structure. The stripe width was 100 μm in this structure, and beside the stripe a SiO_2 layer was deposited to hinder the injected current from overflowing. To improve the COD level, NAW structures were made near each facet to avoid the light absorption of the facets. The cavity length L_c of the LDs was 900 μm and the window region was 25 μm per facet. Ohmic contacts were formed with Ti-Pt-Au for the p-side and Au-Ge-Ni for the n-side. An anti-reflection (5%) coating and a high-reflection (95%) coating were formed on the front and rear facets, respectively. The LD chip was mounted on a Cu heat sink in the p-side down configuration. For comparison, we also fabricated the conventional LD without any window-processing near each facet. Hereafter, the above two types of LDs were called the NAW LD and the conventional LD, respectively.

The two types of LDs devices were tested for the continuous-wave (CW) light output power versus current (L-I), the COD level, the threshold current $I_{\rm th}$, the lasing wavelength, and the far field pattern. In the experiment we found that most of the above characteristics except the CW L-I and the COD level did not have any changes. For the two types of LDs, $I_{\rm th}$ was 0.30 A. At 0.6 W, the wavelength was 670.1 nm, and the beam divergences perpendicular $\theta_\perp$ and parallel $\theta_\parallel$ to the junction plane (full-width at half-maximum power) were 39.1° and 9.3°, respectively. Figure 4 shows the CW L-I characteristics and the COD levels for the two types of LDs. The COD power increased from 0.75 W of the conventional LD to 1.40 W of the NAW LD. The COD power of the NAW LD was higher than that of the conventional LD by 86.7%.

Xu *et al.*[16] reported the COD power (45 mW) of the LDs with Zn-diffused window, higher 80% than that of

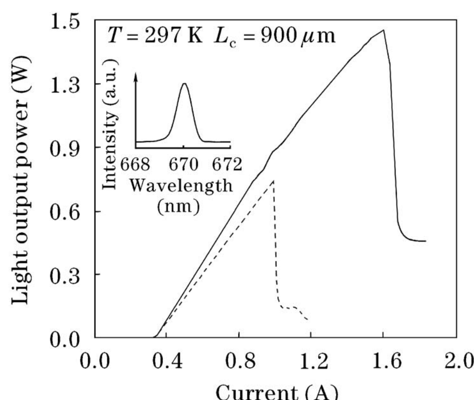

Fig. 4. *L-I* characteristics and the COD levels for the NAW LD (solid curve) and the conventional LD (dashed curve). The inset shows the lasing spectrum, and the wavelength is 670.1 nm at 0.6 W.

the conventional LDs. For explaining the increase of the COD power, the following three points should be noticed. First, compared with Ref. [16], the width of the active region increased from 3.5 to 100 μm, and the cavity length from 600 to 900 μm. These two points expanded the current-injected region and the light-gain region. Second, the $Al_{0.5}In_{0.5}P$ cladding layers decreased the current leakage and the light absorption more effectively than $(Al_xGa_{1-x})_{0.5}In_{0.5}P$ material, because $Al_{0.5}In_{0.5}P$ material has wider energy gap, $E_g = 2.286$ meV[17]. Finally, the important point affecting the COD power is the gap energy shift induced by Zn diffusion. In this letter, it was found that the energy shift of 24.7 meV, lower than 96 meV in Ref. [16], is reasonable for GaInP/AlGaInP LDs. Actually, the larger gap energy shift goes with the more Zn atoms diffused into LDs structures. In the diffusion process, the Zn diffusion can affect the doping concentration in the cladding layers while these Zn atoms serve as the non-radiation recombination center. The former decreases the electron confinement, and the latter increases the light absorption.

In conclusion, LP-MOCVD method had been used to grow the high power GaInP/AlGaInP laser diode wafers. In order to improve devices COD power, the NAW structure was made using Zn diffusion-induced QWI technique. The COD power of the NAW LD was 1.40 W, higher than that of the conventional LD by 86.7%. These results showed that the NAW structure could improve output power of LD effectively.

The authors would like to thank Guohong Wang for the growth of the GaInP/AlGaInP material, and Qiang Gui for assistance in experimental work. The research was supported by the National Natural Science Foundation of China under Grant No. 60236030. K. Zheng's e-mail address is zhengkai@semi.ac.cn.

References

1. N. Lichtenstein, R. Winterhoff, F. Scholz, H. Schweizer, S. Weiss, M. Hutter, and H. Reichl, IEEE J. Sel. Top. Quantum Electron. **6,** 564 (2000).
2. K. Masumoto, I. Yamada, H. Tanaka, Y. Fujise, and K. Hashimoto, Lasers in Medical Science **18,** 134 (2003).
3. M. Sagawa, K. Hiramoto, T. Toyonaka, T. Kikawa, S. Fujisaki, and K. Uomi, Electron. Lett. **32,** 2277 (1996).
4. F. G. Gfeller, P. Buchmann, P. W. Epperiein, H. P. Meier, and J. P. Reithmaier, J. Appl. Phys. **72,** 2131 (1992).
5. T. Shibutani, M. Kume, K. Hamada, H. Shimizu, K. Itoh, G. Kano, and I. Teramoto, IEEE J. Quantum Electron. **23,** 760 (1987).
6. H. Hamada, M. Shono, S. Honda, R. Hiroyama, K. Matsukawa, K. Yodoshi, and T. Yamaguchi, Electron. Lett. **27,** 661 (1991).
7. S. Kamiyama, Y. Mori, Y. Takahashi, and K. Ohnaka, Appl. Phys. Lett. **58,** 2595 (1991).
8. H. Naito, M. Kume, K. Hamada, H. Shimizu, and G. Kano, IEEE J. Quantum Electron. **25,** 1495 (1989).
9. J. E. Ungar, N. S. K. Kwong, S. W. Oh, J. S. Chen, and N. B. Chaim, Electron. Lett. **30,** 1766 (1994).
10. A. Shima, H. Tada, K. Ono, M. Fujiwara, T. Utakouji, T. Kimura, M. Takemi, and H. Higuchi, IEEE Photon. Technol. Lett. **9,** 413 (1997).
11. Y. Ueno, K. Endo, H. Fujii, K. Kobayashi, K. Hara, and T. Yuasa, Electron. Lett. **26,** 1726 (1990).
12. K. Itaya, M. Ishikawa, G. Hatakoshi, and Y. Uematsu, IEEE J. Quantum Electron. **27,** 1496 (1991).
13. H. C. Ko, M. W. Cho, J. H. Chang, and M. Yang, Appl. Phys. A **68,** 467 (1999).
14. H. Hamada, M. Shono, S. Honda, R. Hiroyama, K. Yodoshi, and T. Yamaguchi, IEEE J. Quantum Electron. **27,** 1483 (1991).
15. W. D. Laidig, N. Holonyak, M. D. Camras, K. Hess, J. J. Coleman, P. D. Dapkus, and J. Bardeen, Appl. Phys. Lett. **38,** 776 (1981).
16. Y. Xu, Q. Cao, X. Zhu, G. Yang, Q. Gan, G. Song, L. Guo, Y. Li, and L. Chen, Chin. Opt. Lett. **2,** 647 (2004).
17. I. Vurgaftman, J. R. Meyer, and L. R. Ram-Mohan, J. Appl. Phys. **89,** 5815 (2001).